Resonance Frequency and Stiffness of Magnetic Bead Chain in Magnetic Field

Hiroyuki Kawamoto, Nobuyuki Nakayama and Satoshi Yamada
Department of Mechanical Engineering, Waseda University
Shinjuku, Tokyo, Japan

Abstract

Experimental, theoretical, and numerical investigations have been carried out to evaluate resonance frequency and stiffness of a magnetic bead chain in the magnetic filed. Chains formed on a solenoid coil were vibrated by the sine-wave excitation and impact methods and the resonance frequency was deduced. It showed little dependency on the magnetic flux density and the bead diameter, because both the equivalent stiffness and the chain length were large in accordance with the increase of the magnetic flux density. These characteristics were confirmed by a theoretical consideration based on an assumption of potential energy minimization and a numerical calculation with the Distinct Element Method. Stiffness of the chain was directly measured by observation of chain deflection in inclined gravitational field and it also confirmed the dynamically deduced characteristics. It was concluded that the resonance frequency was 20–60 Hz and the static stiffness at the top of the chain was 10^{-4}–10^{-2} N/m. The investigation is utilized for the improvement of the two-component magnetic blush development subsystem in electrophotography.

Introduction

A magnetic brush development system[1,2] is most widely used for high-speed color laser printers. A typical schematic of this system is illustrated in Fig. 1. Magnetic carrier beads with electrostatically attached toner particles are introduced into the vicinity of a rotatory sleeve with a stationary magnetic roller inside it. Carrier beads form chains on a sleeve by virtue of the magnetic field. Tips of chains touch a photoreceptor surface at the development area and toner particles on chains move to electrostatic latent images on a photoreceptor to form real images. Carrier chains play an important role in this development step. In order to realize high quality imaging, it is necessary to clarify the relationship between static and dynamic characteristics of formed chains and design parameters, such as the magnetic flux density and properties of carriers.

Statics of chains has been already investigated and it has been clarified how chain configuration is determined in the magnetic field.[3] It is also important to clarify resonance frequency and stiffness of the chain in the magnetic field. Hard chains might cause a stripe image defect and on the other hand a "bead-carry-out" might take place if chains were too soft. In this study, following the static investigation,[3] experimental, theoretical, and numerical investigations have been carried out on dynamics of the chain.

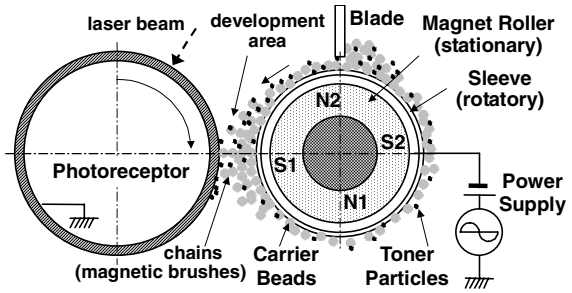

Figure 1. Magnetic brush development system in a laser printer.

Experimental Procedure

Three experimental methods have been employed to measure the resonance frequency and to evaluate the stiffness of the chain. They are a sine-wave excitation method, an impact test, and a static inclination method.

Sine-Wave Excitation

Figure 2 and Figure 3 show an experimental set-up and its photograph, respectively, to measure the resonance frequency of the chain. A solenoid coil with carrier chains was mounted on a shaker (Shinken Co., G14-818), and vibration of chains was observed through a microscope camera (Keyence Corp., VH-7000). The coil was 55 turns of ϕ 0.5 mm copper wire and the dimensions are ϕ 30 mm inner diameter, ϕ 38 mm outer diameter, and 33.5 mm length. Five kinds of spherical carriers were used for experiments. These are soft magnetic material made by the polymerization method with 18, 35, 55, 88, and 107 μm in diameter, 3500–3620 kg/m^3 volume density, and 4.2–4.7 in relative magnetic permeability (Toda Kogyo Corp.). Photograph of one of them (107 μm in diameter) is shown in Fig. 4(a). Carrier beads were initially arranged at the center of a plastic plate on a coil end in a ϕ 10 mm area. Axial magnetic flux density B' along the center axis of the coil was measured by a separate experiment and approximated by $B'(z) = B_0(1-cz)$, where B_0 and c (= 66.87 1/m) are constants and z

(m) is the axial coordinate (z = 0 at the surface of the end plate on which carrier beads were mounted). B_0 is proportional to the coil current with a proportional constant 0.00616 T/A. This approximation was confirmed by theoretical and FEM calculations. The coil was excited in two directions: one is axial and another is radial as shown in Fig. 2. The shaker was operated with the sine wave and the frequency was swept up and down from 10 to 90 Hz at 1.5 Hz/s speed-up/down rate.

The resonant frequency of bulk chains was not single but it distributed in a wide range, because characteristics of chains were not identical but bulk chains contained long and short, as shown in Fig. 4(b), and softly and hardly connected chains. This feature made the determination of the resonance frequency very difficult. In this experiment, averaged values observed by four persons at three times were adopted as representatives. It should be emphasized that data contained fairly large error.

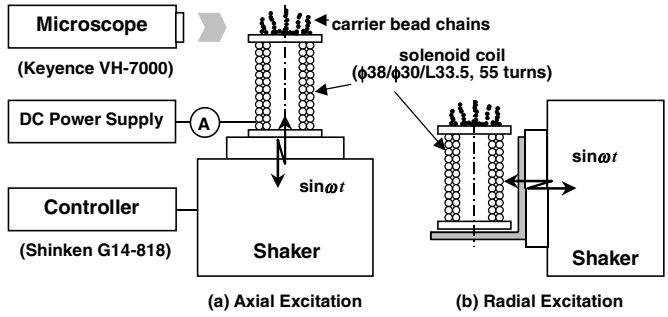

Figure 2. Experimental set-up of sine-wave excitation method to measure resonant frequency of bead chains in magnetic field.

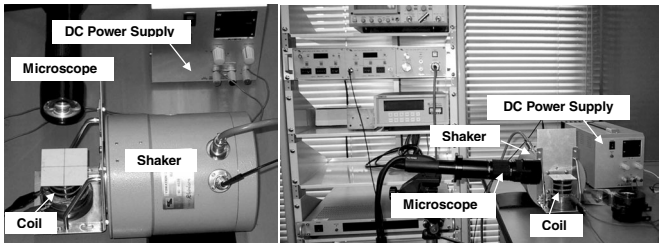

Figure 3. Photographs of experimental set-up of sine-wave excitation method.

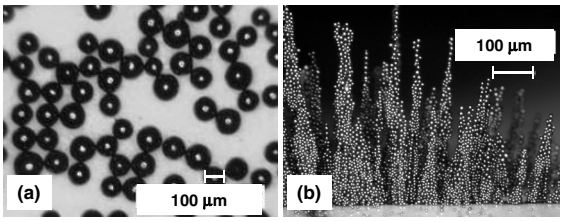

Figure 4. (a) Magnetic carrier beads (107 μm diameter) and (b) chains in magnetic field (88 μm diameter, in 3 A field).

Impact Test

An impact method was also employed to determine the resonance frequency more exactly than the forced vibration method. A set-up is shown in Fig. 5. Free vibration response of bulk chains measured by a laser displacement meter (Keyence Corp., LK-2000) was introduced to an FFT analyzer and then the resonance frequency was specified. The solenoid coil and carrier particles are common with those used in the sine-wave excitation method.

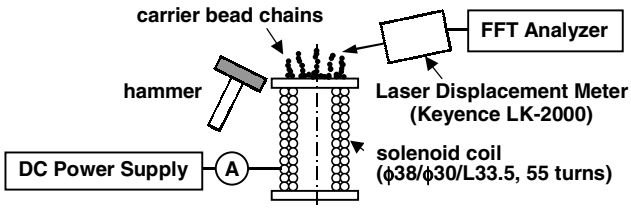

Figure 5. Experimental set-up of impact method to measure resonance frequency of bead chains in magnetic field.

Static Inclination Method

Chains are not exactly directed parallel to the magnetic flux, if the flux inclines to the gravity.[3] The static stiffness of the chain was estimated from chain inclinations in inclined magnetic fields. Fig. 6 is an experimental set-up to measure the inclination in the intentionally inclined field. The solenoid coil with bead chains was mounted on a θ-stage and then slant angles of chains were measured by the microscope. The solenoid coil and carrier particles were also common with those used in the sine-wave excitation method.

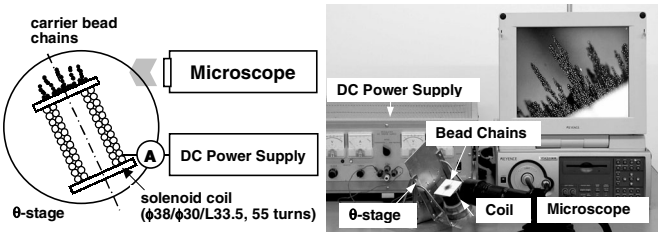

Figure 6. Experimental set-up of static inclination method to evaluate static stiffness of bead chains in magnetic field.

Experimental Results

Axial Sine-Wave Excitation

The axial sine-wave excitation experiment was conducted under a condition of a constant magnitude (0.4 mm) of the shaker vibration. Although excitation acceleration exceeded 1 G (9.8 m/s^2) over 25 Hz, chains did not break nor jump, because magnetic attractive force was larger than axial excitation force. Radial resonant vibration was observed even though chains were excited in the axial direction, because the excitation was not exactly axial but it contained a

radial component and chains were not perpendicular to the axial direction except at the center. Fig. 7 shows observed resonant frequency. Lower and upper limits of the vibration occurrence were cited 'lower' and 'upper,' respectively. Although the resonant frequency laid in wide range and small hysteresis existed, it roughly suggested that the resonant frequency did not depend on the magnetic flux density. Fig. 8 shows a relationship between the particle size and the averaged resonant frequency. The particle size also did not influence the resonance frequency.

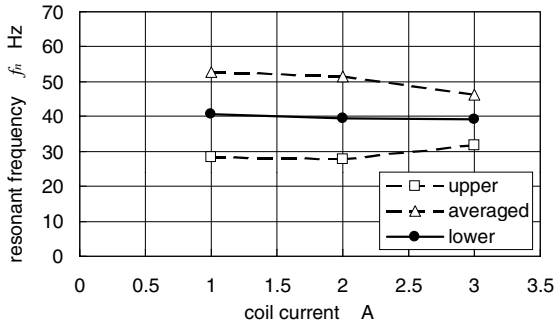

Figure 7. Resonant frequency measured by axial excitation method. (88 μm diameter, 0.05 g @ ϕ 10 mm)

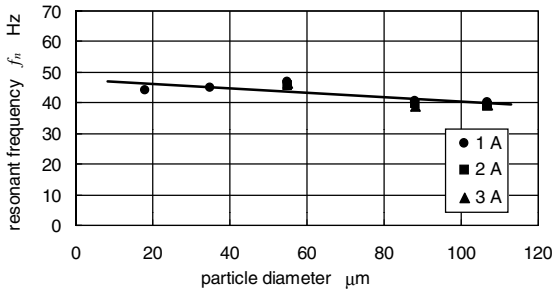

Figure 8. Relationship between particle size and resonant frequency. (0.05 g @ ϕ 10 mm)

Equivalent stiffness of the chain was evaluated from experimental data. The chain was assumed to be a cone shape and an equivalent mass of the chain m_c was estimated from the measured chain length and bottom width. These are shown in Fig. 9. Bulk density of the chain was assumed to be 0.5 from a separate experiment. The equivalent stiffness was calculated from $m_c(2\pi f_n)^2$ and shown in Fig. 10, where f_n is the measured resonant frequency shown in Fig. 7. It is recognized form Fig. 10 that the stiffness of the chain was high in the high magnetic field. This is because the magnetic force between beads is high in the high magnetic field. However, because both the mass and the stiffness of the chain increase with the increase of the magnetic flux density, the resonance frequency is almost independent on the magnetic flux density.

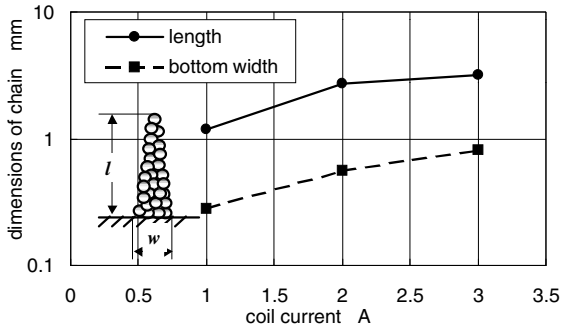

Figure 9. Characteristic sizes of chain. (88 mm diameter, 0.05 g @ ϕ 10 mm)

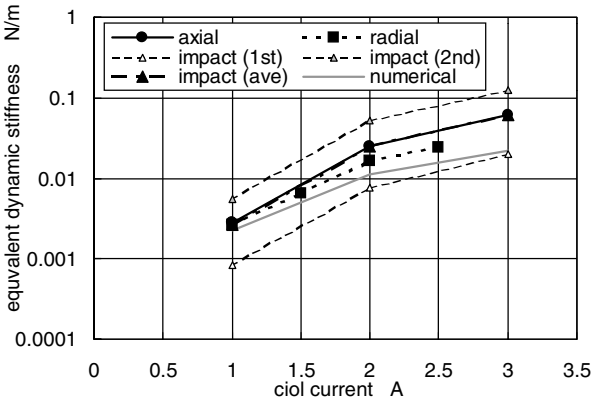

Figure 10. Equivalent dynamic stiffness of chain.

Radial Sine-Wave Excitation

The radial sine-wave excitation experiment was conducted under almost the same conditions except that a constant acceleration (1–3 m/s^2) scheme was employed. Measured resonant frequencies of the lower limit are shown in Fig. 11 and 12. Because the chain shifted laterally at high excitation frequency, the upper limit of the resonant frequency could not be observed. Repulsive force between adjacent chains[4] is the cause of the lateral movement. In any case, although the resonant frequency was slightly decreased with the increase of the magnetic field and the particle diameter, the dependencies are small. These characteristics agreed qualitatively with those of the axial excitation experiment.

Equivalent stiffness of the chain was deduced with the same procedure described in the previous section. The result was added in Fig. 10. The estimated stiffness from the radial excitation was similar with that from the axial excitation.

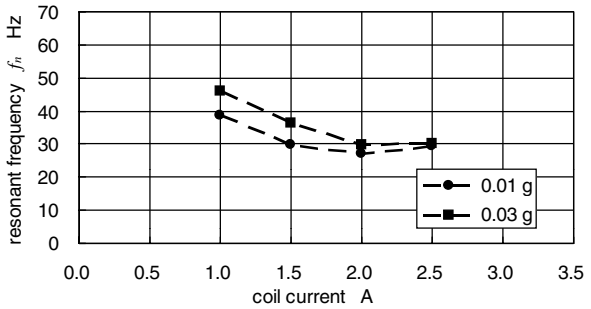

Figure 11. Lower limit of resonant frequency measured by radial excitation method. (88 μm diameter)

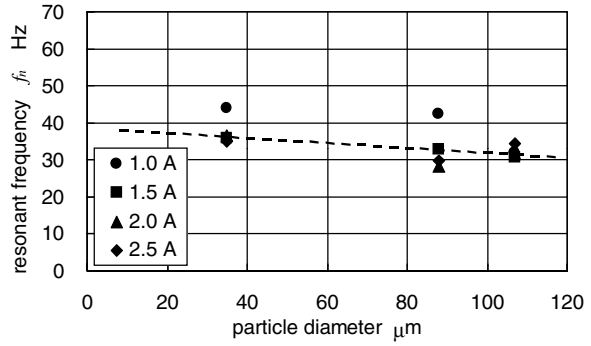

Figure 12. Relationship between particle size and lower limit of resonant frequency. (average of 0.01 g and 0.03 g @ ϕ 10 mm)

Free Vibration (Impact Test)

Figure 13 shows an example of a free vibration response by the impact method and Fig. 14 is a spectrum, an averaged value of 30 spectra measured at the same experimental conditions. A spectrum without current passage is added in Fig. 14 to eliminate resonance frequencies without the magnetic field and to identify resonance frequencies of formed chains at a certain magnetic field. Fig. 15 summarizes resonance frequencies as a parameter of the magnetic flux density (coil current), the bead diameter, and the particle weight to surface loading. It is clearly recognized that two major resonance frequencies, about 20 Hz and 60 Hz, exist and both are almost irreverent with the magnetic flux density, the bead diameter, and the particle weight to surface loading. Although the vibration modes are not clear, the effect of parameters coincided with results of the forced vibration method.

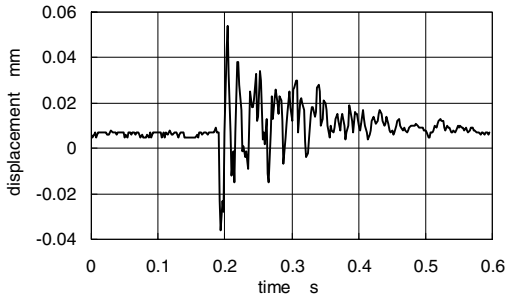

Figure 13. Free vibration response of bulk chains. (3 A, 35 μm diameter, 0.05 g @ ϕ 10 mm)

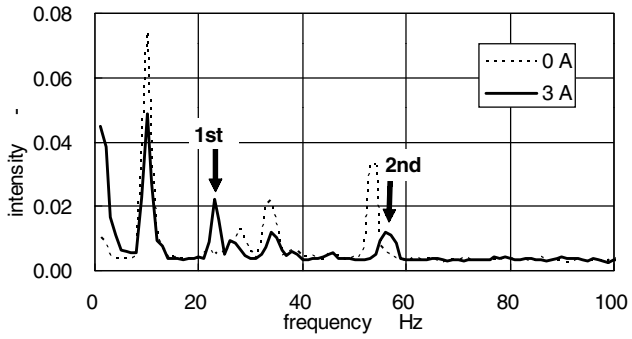

Figure 14. Spectrum of free vibration response of bulk chains.

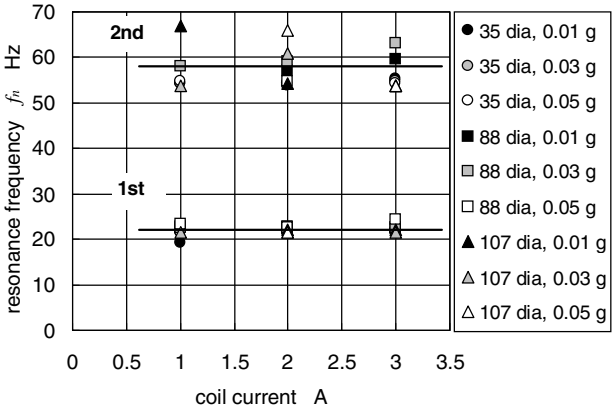

Figure 15. Resonance frequency of bulk chains in magnetic field.

The equivalent stiffness of the chain was also deduced with the same procedure described in the axial excitation section and the result is added in Fig. 10. The averaged stiffness from the impact test was good agreement with those from the axial and radial excitations.

Static Inclination in Inclined Field

Slant angle of the chain in the inclined magnetic field is shown in Fig. 16. It is clearly recognized that the chain angle was enlarged by the gravity and it was larger than that of the magnetic flux. Although the chain was collapsed when the angle of the magnetic flux to the gravity was larger than a threshold, 50 degree in the case of Fig. 16, the chain angle was almost linear with respect to the flux angle. Fig. 17 is the rate of the increase in the angle, $100(\phi-\theta)/\theta$. The chain inclination was highly increased in the low magnetic field but it was almost parallel to the flux in the high magnetic field, more than 4 A coil current, because the chain became stiff in the high magnetic field.

The static stiffness of the chain was calculated from these inclination data. The stiffness at the top of the chain k is determined from a momentum balance, if the chain is assumed to be a line.

$$k = \frac{\pi \rho g a^2}{12 c \theta} \sin\theta, \qquad (1)$$

where ρ is the density of the carrier bead, g is the gravitational constant, a is the diameter of the bead, θ is the angle of the magnetic flux to the gravity, and c is a proportional constant of the increase. The estimated stiffness is shown in Fig. 18. The stiffness is large in high magnetic field. This characteristic is common with that deduced from dynamics, however, two differences are evident between the dynamic stiffness summarized in Fig. 10 and the static stiffness in Fig. 18. One is a magnitude. The static stiffness was at least one order of magnitude smaller than the dynamic stiffness. One evident reason is that the static stiffness is defined at the top of the chain whereas the dynamic stiffness corresponds to the lateral vibration and it was deduced from the simple total mass without taking account of a vibration mode. Another possible reason is that the static deflection includes that due to the rotation of beads although lateral deformation is major for the dynamic stiffness. Another difference between static and dynamic is the effect of the bead diameter. The static stiffness was highly dependent on the bead diameter. This is not the case for the dynamic stiffness. One possible reason is also the contribution of the bead rotation in the case of the static deflection.

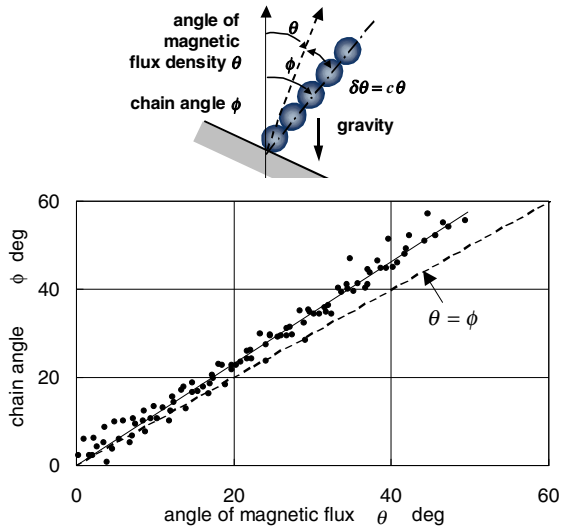

Figure 16. Chain angle in inclined magnetic field. (2 A, 35 μm diameter, 0.05 g @ φ 10 mm)

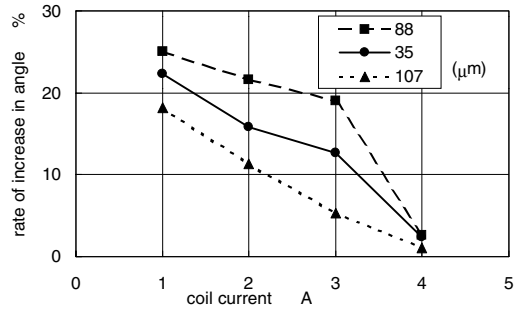

Figure 17. Rate of increase in angle. (0.05 g @ φ 10 mm)

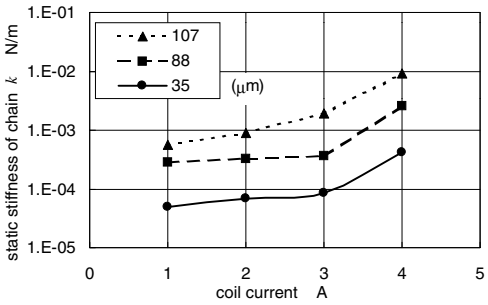

Figure 18. Static stiffness at top of chain.

Theoretical

It is assumed that chain lengths are determined to minimize its total potential energy given by the sum of magnetic energy U_m and gravitational energy U_k.

$$U_m = -\frac{1}{2}\sum_{j=1}^{N} \boldsymbol{m}_j \cdot \boldsymbol{B}'_j, \quad U_k = g\sum_{J=2}^{N} m_{bj}\left(\sum_{k=1}^{N-1} a_k + \frac{a_N}{2}\right), \tag{2}$$

where N is a total number of beads and m_{bj} is the mass of j-th bead. The magnetic moment $\boldsymbol{m}_j$ at the position of the j-th particle is

$$\boldsymbol{m}_j = \frac{4\pi}{\mu_0}\frac{\mu-1}{\mu+2}\frac{a^3}{8}\boldsymbol{B}'_j + \frac{\mu-1}{\mu+2}\frac{a^3}{8}\sum_{\substack{k=1\\k\neq j}}^{N}\left[3\frac{(\boldsymbol{m}_k\cdot\boldsymbol{r}_{kj})}{r_{kj}^5}\boldsymbol{r}_{kj} - \frac{\boldsymbol{m}_k}{r_{kj}^3}\right], \tag{3}$$

where μ_0 is the magnetic permeability of free space and μ is the relative permeability of beads. The first term in the right hand side of Eq. (3) is due to the applied magnetic field by the coil and the second term is generated at the j-th bead by the field due to dipoles of other beads. Although the assumption is not exactly right because the system is not a potential but irreversible, it roughly approximates static chain formation in the magnetic field.[3] Based on this concept it is also assumed, as a first order approximation, that the equivalent stiffness of the chain is proportional to the total potential energy per a bead. Fig. 19 shows the calculated relative resonance frequency, where beads are assumed to be connected along a straight line in vertical. Although the resonance frequency is not constant with respect to the magnetic flux density and the bead diameter, the dependencies are small.

Numerical Simulation

Numerical Method

Two-dimensional Distinct Element Method (DEM) was used in the numerical simulation of the dynamic behavior of the magnetically formed chain. In the calculation the momentum equations are solved with three degrees of freedom, (u, v, φ) for each bead j, where (u, v) are displacements in the Cartesian coordinates and φ is a rotational angle. In this study, mechanical interaction force and moment, $\boldsymbol{F}_c$ and $\boldsymbol{M}_c$, the magnetic force and moment, $\boldsymbol{F}$ and $\boldsymbol{M}$, air drag, and the

gravity are considered in the equations but the effect of rolling friction and van der Waals force are neglected.

$$m_{bj}\ddot{\boldsymbol{x}} = \boldsymbol{F}_{cj} + \boldsymbol{F}_j + 6\pi\eta\dot{\boldsymbol{x}}_j + m_{bj}\boldsymbol{g},\ I_j\ddot{\varphi} = M_{cj} + M_j,\ \boldsymbol{x} = (u, v) \quad (4)$$

where I is an inertia of the particle and η is a viscosity. The mechanical interaction force is calculated by the Hertz's formula. The magnetic force and the rotational moment of the j-th bead with the magnetic moment $\boldsymbol{m}_j$ are given by the following expressions under the assumption that each bead behaves as a magnetic dipole placed at the center of the magnetized bead.

$$\boldsymbol{F}_j = (\boldsymbol{m}_j \cdot \nabla)\boldsymbol{B}_j, \quad \boldsymbol{M}_j = \boldsymbol{m}_j \times \boldsymbol{B}_j. \quad (5)$$

The magnetic flux density $\boldsymbol{B}_j$ at the position of the j-th bead is

$$\boldsymbol{B}_j = \boldsymbol{B}'_j + \frac{\mu_0}{4\pi}\sum_{\substack{k=1 \\ k\neq j}}^{N}\left[3\frac{(\boldsymbol{m}_k \cdot \boldsymbol{r}_{kj})}{r_{kj}^5}\boldsymbol{r}_{kj} - \frac{\boldsymbol{m}_k}{r_{kj}^3}\right] \quad (6)$$

Although the actual chain was a cone or tower shape, a single row of beads was assumed in the calculation to evaluate the effect of the magnetic flux density and the chain length separately. Calculation conditions are; Young's modulus of beads = 10 GPa, Young's modulus of plate = 100 GPa, Poisson's ratio = 0.3, and friction coefficient = 0.2. Diameter, particle weight to surface loading, and magnetic permeability of beads were adjusted with the measured.

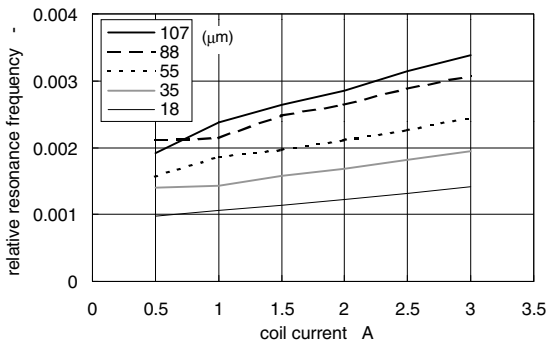

Figure 19. Relative resonance frequency of chain in magnetic field based on the concept of potential energy minimization.

Numerical Results

A step force was applied to the chain and the response of the chain deformation was calculated. The bottom bead was fixed to the plate to prevent lateral shift of the chain and the magnitude of acceleration was adjusted not to break down the chain. One example of calculation was shown in Fig. 20 and 21. Fig. 20 is a time-step variation of the chain profile and Fig. 21 is the vibration response of the top bead. Because the bead row was assumed to be a line, a slope was highest at the lowest bead and therefore the mode of vibration was not exactly the same with that of the actual chain. The resonance frequency was 41.7 Hz in this case.

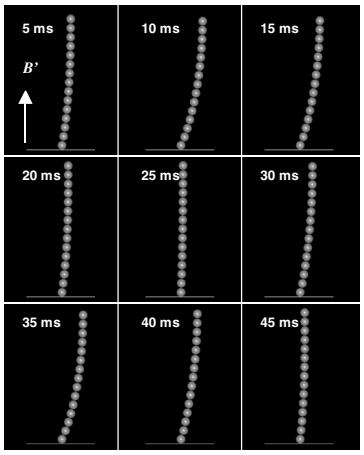

Figure 20. Time variation of chain profile. (15 beads, 3 A, 1.7 m/s² acceleration)

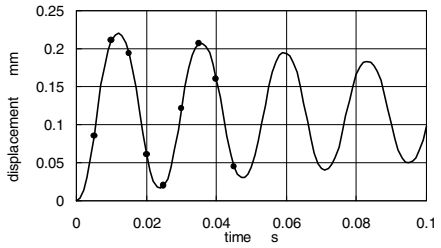

Figure 21. Horizontal displacement of top bead. Calculation conditions are common with those of Figure 20.

Parametric calculation was conducted to examine effects of the magnetic flux density and the bead length. Fig. 22 shows vibration responses of 5-bead chain in 1, 2, and 3 A coil-current fields and Fig. 23 is the deduced stiffness of the chain. Here, the total mass of the line chain was adapted to calculate the frequency. Since the chain for the calculation is not a tree shape but assumed to be the simple line, the magnitude of the deduced stiffness does not coincide with the measured shown in Fig. 10. However, it is qualitatively recognized that the frequency and therefore the stiffness become higher in the higher magnetic flux density, if the number of beads is constant.

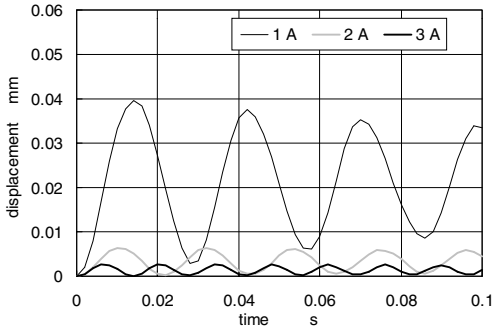

Figure 22. Horizontal displacements of 5-bead chain in different magnetic field.

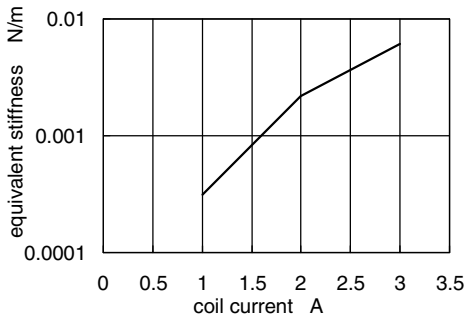

Figure 23. Equivalent stiffness of 5-bead chain.

The next calculation is to examine effect of bead length. Fig. 24 is vibration responses of chains that consist of 3, 5, and 7 beads in the common field (1 A coil current) and Fig. 25 is the deduced stiffness. The frequency and therefore the stiffness are obviously low when the chain is long.

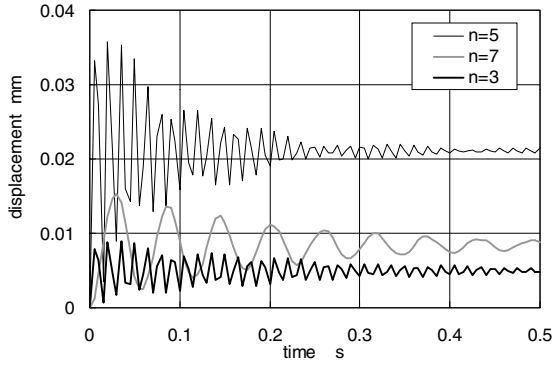

Figure 24. Horizontal displacements of chains that consist of different number of beads in the common magnetic field. (1 A)

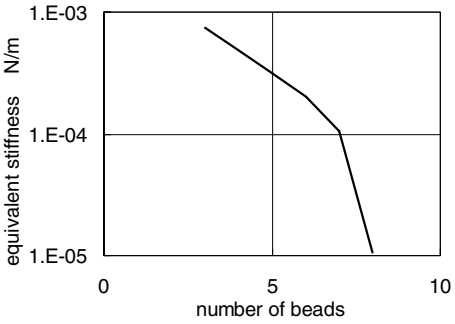

Figure 25. Equivalent stiffness of chain in common field. (1 A)

Combining two calculation results on the effect of the magnetic flux density and the chain length, we can deduce the resonance frequency of the chain that consists of a realistic number of beads based on the experimental result.[3] Fig. 26 shows the comparison of the calculated and measured resonance frequency. Numerical calculation was conducted with the half-length chain corresponding to those of Fig. 9 to avoid dynamic break down of chain. This occurred because the single row of beads was assumed whereas the actual chain was the stable cone shape. In any case, the calculated resonance frequency is almost independent on the magnetic flux density. This qualitatively agrees with the measured and theoretical results.

Finally, the dynamic stiffness was deduced and added in Fig. 10 to compare directly with measured. The calculated was the same order with dynamically measured results.

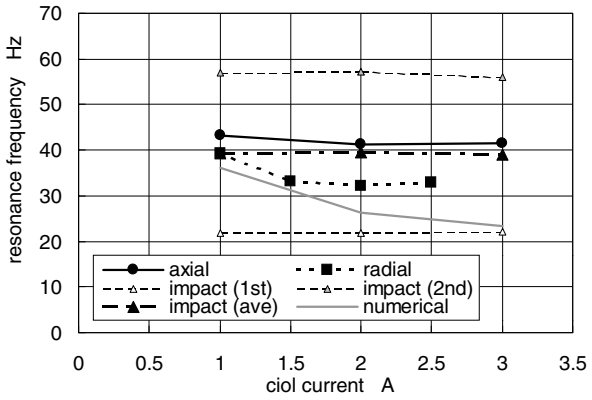

Figure 26. Calculated and measured resonance frequency. (88 μm diameter)

Concluding Remarks

Experimental, theoretical, and numerical studies have been carried out on statics and dynamics of a magnetic bead chain in the magnetic filed to utilize for the improvement of the two-component magnetic blush development subsystem in electrophotography. The following were deduced from the investigation.

(1) The resonance frequency of the carrier bead chain was 20–60 Hz and it was almost irrelevant with the magnetic flux density, the bead diameter, and particle weight to surface loading.

(2) The static stiffness at the top of the chain was 10^{-4}–10^{-2} N/m. It was large in the high magnetic field or for large diameter beads.

Further investigation is being conducted on the measurement of the static stiffness by a sophisticated method and three-dimensional DEM calculation for realistic cone-shape chains.[5]

Acknowledgement

The authors would like to express their thanks to the Ministry of Education, Science and Culture of Japan for the financial support, to Toda Kogyo Corp. for supplying carrier beads, and to J. Wiphut (Bank of Thailand), N. Sukou (Waseda Univ.), and A. Sasakawa (Chiba Prefectural Government) for their help of carrying out experiments.

References

1. E. M. Williams, *The Physics and Technology of Xerographic Processes*, Krieger Publishing, FL (1993).
2. L. B. Schein, *Electrophotography and Development Physics* (Revised Second Edition), Laplacian Press, CA (1996).
3. N. Nakayama, H. Kawamoto and M. Yamaguchi, Statics of Magnetic Bead Chain in Magnetic Field, *J. Imaging Sci. Technol*. (submitted).
4. R. S. Paranjpe and H. G. Elrod, Stability of chains of permeable spherical beads in an applied magnetic field, *J. Appl. Phys*., 60 (1986), 418-422.
5. N. Nakayama, H. Kawamoto, H. Yamada and A. Sasakawa, Statics of Electromagnetic Bead Chains in Electromagnetic Field, *IS&T's NIP18: 18th International Conf. on Digital Printing Technologies*, p. 742 (2002).

Biography

Hiroyuki Kawamoto holds a BS degree in Electrical Engineering from Hiroshima Univ. (1972) and a Dr. degree in Mechanical Engineering from Tokyo Institute of Technology (1983). From 1972 to 1991 he was a Senior Engineer at the Nuclear Division of Hitachi Ltd. In 1991 he moved to Fuji Xerox, and had been engaged in the research of electrophotography as a Research Fellow. In 1999 he left Fuji Xerox and he is now a professor of Waseda Univ. His awards include the Japan Society of Mechanical Engineers Young Scientist Award (1984), the 7th International Microelectronics Conf. Best Paper Award (1992), the Japan Institute of Invention and Innovation Patent Award (1993), and the 10th International Symposium on Applied Electromagnetics and Mechanics Award for Outstanding Presentation Paper (2001). He was selected a Fellow of the IS&T in 1999.